www.elsevier.com/locate/jep

Qualitatively and Quantitatively Investigating the Regulation of Intestinal Microbiota on the Metabolism of Panax notoginseng saponins

Jingcheng Xiao, Huimin Chen, Dian Kang, Yuhao Shao, Boyu Shen, Xinuo Li, Xiaoxi Yin, Zhangpei Zhu, Haofeng Li, Tai Rao, Lin Xie, Guangji Wang, Yan Liang

PII: S0378-8741(16)30818-2
DOI: http://dx.doi.org/10.1016/j.jep.2016.09.027
Reference: JEP10427

To appear in: *Journal of Ethnopharmacology*

Received date: 23 June 2016
Revised date: 21 August 2016
Accepted date: 13 September 2016

Cite this article as: Jingcheng Xiao, Huimin Chen, Dian Kang, Yuhao Shao Boyu Shen, Xinuo Li, Xiaoxi Yin, Zhangpei Zhu, Haofeng Li, Tai Rao, Lin Xie Guangji Wang and Yan Liang, Qualitatively and Quantitatively Investigating the Regulation of Intestinal Microbiota on the Metabolism of Panax notoginseng saponins, *Journal of Ethnopharmacology* http://dx.doi.org/10.1016/j.jep.2016.09.027

Qualitatively and Quantitatively Investigating the Regulation of Intestinal Microbiota on the Metabolism of Panax notoginseng saponins

Jingcheng Xiao[1], Huimin Chen[1], Dian Kang, Yuhao Shao, Boyu Shen, Xinuo Li, Xiaoxi Yin, Zhangpei Zhu, Haofeng Li, Tai Rao, Lin Xie, Guangji Wang[**], Yan Liang[*]

Key Lab of Drug Metabolism & Pharmacokinetics, State Key Laboratory of Natural Medicines, China Pharmaceutical University, Tongjiaxiang 24, Nanjing 210009, China

[*]Corresponding author. Tel. : +86 25 83271060; fax: +86 25 83271060. liangyan0679@hotmail.com.

[**]Corresponding author. Tel.: +86 25 83271128; fax: +86 25 83302827.

Abstract

ETHNOPHARMACOLOGICAL RELEVANCE

Intestinal microflora plays crucial roles in modulating pharmacokinetic characteristics and pharmacological actions of active ingredients in traditional Chinese medicines (TCMs). However, the exact impact of altered intestinal microflora affecting the biotransformation of TCMs remains poorly understood.

AIMS OF THE STUDY

This study aimed to reveal the specific enterobacteria which dominate the metabolism of panax notoginseng saponins (PNSs) via exploring the relationship between bacterial community structures and the metabolic profiles of PNSs.

MATERIALS AND METHODS

2, 4, 6-Trinitrobenzenesulphonic acid (TNBS)-challenged and pseudo germ-free (pseudo GF) rats,

[1] These two authors contributed equally to this work.

which prepared by treating TNBS and antibiotic cocktail, respectively, were employed to investigate the influence of intestinal microflora on the PNS metabolic profiles. Firstly, the bacterial community structures of the conventional, TNBS-challenged and pseudo GF rat intestinal microflora were compared via 16S rDNA amplicon sequencing technique. Then, the biotransformation of protopanaxadiol-type PNSs (ginsenoside Rb1, Rb2 and Rd), protopanaxatriol-type PNSs (ginsenoside Re, Rf, Rg1 and notoginsenoside R1) and Panax notoginseng extract (PNE) in conventional, TNBS-challenged and pseudo GF rat intestinal microbiota was systematically studied from qualitative and quantitative angles based on LC-triple-TOF/MS system. Besides, glycosidases (β-glucosidase and β-xylosidase), predominant enzymes responsible for the deglycosylation of PNSs, were measured by the glycosidases assay kits.

RESULTS

Significant differences in the bacterial community structure on phylum, class, order, family, and genera levels were observed among the conventional, TNBS-challenged and pseudo GF rats. Most of the metabolites in TNBS-challenged rat intestinal microflora were identified as the deglycosylation products, and had slightly lower exposure levels than those in the conventional rats. In the pseudo GF group, the peak area of metabolites formed by loss of glucose, xylose and rhamnose was significantly lower than that in the conventional group. Importantly, the exposure levels of the deglycosylated metabolites were found have a high correlation with the alteration of glycosidase activities and proteobacteria population. Several other metabolites, which formed by oxidation, dehydrogenation, demethylation, etc, had higher relative exposure in pseudo GF group, which implicated that the up-regulation of Bacteroidetes could enhance the activities of some redox enzymes in intestinal microbiota.

CONCLUSION

The metabolism of PNSs was greatly influenced by intestinal microflora. Proteobacteria may affect the deglycosylated metabolism of PNSs via regulating the activities of glycosidases. Besides, up-regulation of Bacteroidetes was likely to promote the redox metabolism of PNSs via improving the activities of redox metabolic enzymes in intestinal microflora.

Abbreviations: TCMs：Traditional Chinese medicines; **TNBS:** 2, 4, 6-trinitrobenzenesulphonic acid; **GF:** Germ-free; **PNS:** Panax notoginseng saponins; **PPD:** Protopanaxadiol; **PPT**: Protopanaxatriol; **PNE:** Panax notoginseng extract; **CMMA:** Chemicalome-metabolome matching approach; **LC-MS:** Liquid chromatography-mass spectrometry; **PCA:** Principal component analysis; **SD:** Sprague-dawley; **TOF:** Time of flight. **IDA:** information dependent acquisition

Keywords: Intestinal microflora; Panax notoginseng extract; Panax notoginseng saponin; Glycosidase; Deglycosylation

1. Introduction

Intestinal microflora, a complex ecosystem composed of nearly 10^{14} micro-organisms, is a large and diverse microbial community residing in or passing through the gastrointestinal tract (Gerritsen et al., 2011). Recent literatures have revealed that the intestinal microflora plays an important role in physiological, nutritional, metabolic and immunological processes, and then alter the pharmacokinetics and pharmacological activities, directly and indirectly, particularly towards

orally administered drugs (Wallace et al., 2010; Haiser and Turnbaugh, 2012; Guadamuro et al., 2015). The effects of intestinal microflora on the pharmacokinetics commonly include the biotransformation, bioavailability and biodegradation as well as regulation of the epithelial transporters, etc (Stojancevic et al., 2014). For drug metabolism, the intestinal microflora is mainly involved in reductive and hydrolytic reactions generating non-polar low molecular weight byproducts (Sousa et al., 2008). Besides, hydrolysis of glycosidic linkage, which is catalyzed by the β-glycosidases (β-glucosidase and β-glucuronidase) to release parent compound via hydrolyzing the glycosidic bond of glycoside and glucuronide conjugates, is one of the best-known examples of microbial enzyme activities (De Preter et al., 2011; Stojancevic et al., 2014).

The practice of traditional Chinese medicines (TCMs) plays an important role in disease prevention and treatment for a long historic time, and makes great influence on human health maintenance and reproduction (Tu, 2011). Oral route is the most common and desirable way of TCM administration for chronic treatments after boiling with water to generate decoction (Qiu, 2007; Stojancevic et al., 2014). Pharmacological activities and pharmacokinetic characteristics of the TCM components could be strongly influenced by intestinal bacteria via modifying their bioavailability and metabolic fate (Nicholson et al., 2005; Cui et al., 2016). Thus, understanding the influence of the structure and function of gut microflora on the pharmacokinetics of TCMs might become the first great breakthrough for the development of TCMs. However, recent studies on TCM were only dominated by its phytochemical identification, metabolite screening, pharmacological activities, toxicity, etc, and the underlying mechanisms of gut microbiota mediating the metabolism of components in TCM received less attention (Xie and Leung, 2009; Wang et al., 2012).

Panax notoginseng (Araliaceae), an ancient medicinal plant in China, was popularly used in the prevention and treatment of cardio-cerebrovascular ischemic diseases besides promoting blood clotting, relieving swelling, alleviating pain, etc (Lin et al., 2015; Fan et al., 2016; Yu et al., 2016). The constituents of PNE consist of saponins, polysaccharides, and flavonoids, etc (Jia et al., 2013). To date, more than 70 kinds of PNSs (including ginsenosides and notoginsenosides) have been

isolated and identified from PNE, and most of the PNSs could be divided into two major groups including the protopanaxadiol (PPD) type with sugar moieties attached to the C-3 with or without C-20, and the protopanaxatriol (PPT) type with sugar moieties at C-6 with or without at C-20 (Han et al., 2010; Xing et al., 2015). Among them, PPD type PNSs (ginsenoside Rb1, Rb2, Rd) and PPT type PNSs (ginsenoside Rb1, Rg1, Rd, Re, notoginsenoside R1) account for above 85 % of the total saponins (Xing et al., 2015). In the past decades, the PNSs in PNE were confirmed to be metabolized to secondary glycosides and/or aglycones with higher bioavailability and bioactivity by enzymes in intestinal microflora (Xu et al., 2014; Kim et al., 2015). Not long ago, it was reported that oral bioavailability of ginsenoside Rb1 in diabetic rats was significantly higher than that in normal rats and the rats fed with high-fat diet, and increased Rb1 exposure in diabetic rats was mainly attributed to significantly impaired Rb1 deglycosylation by the intestinal microflora and increased Rb1 absorption in the intestine (Liu et at., 2015). More recently, Zhou et al. revealed that ginsenoside Re could be metabolized to Rg1 and secondary ginsenosides 20(S)-Rg2 by Bacteroides spp., and Lactobacillus spp. & Bacteroides spp. could transform ginsenoside Rc into ginsenosides 20(S)-Rg3 and Rd (Zhou et al., 2016). Although a few studies demonstrated the influence of intestinal bacteria on the pharmacokinetics of ginsenosides in rats, the action of intestinal microflora on the metabolism of PNSs had not been fully investigated yet, and the mechanisms of intestinal microflora on the transformations of notoginsenosides warrant further investigation (Xu et al., 2014; Kim et al., 2015).

The ongoing revolution in high-throughput sequencing continues to open the possibility for characterizing the hidden microbial components of the biosphere (Avershina et al., 2013; Caporaso et al., 2011). To fully investigate the influence of intestinal microflora on the metabolism of PNSs, TNBS-challenged and pseudo GF rats were prepared and employed to explore the relationship between intestinal microflora and PNS metabolic profiles. Firstly, the bacterial community structure of the conventional, TNBS-challenged and pseudo GF rat intestinal microflora were compared via 16S rDNA amplicon sequencing technique. Then the biotransformation of PPD-type PNSs (ginsenoside Rb1, Rb2 and Rd), PPT-type PNSs (ginsenoside Re, Rf, Rg1 and notoginsenoside R1) and PNE in conventional, TNBS-challenged and pseudo GF rat intestinal microbiota were systematically analyzed and compared from

qualitative and quantitative angles. The specific enterobacteria which dominate the metabolism of PNSs were preliminary explored via analyzing the relationship between bacterial community structure and the metabolic profiles of PNSs.

2. MATERIALS AND METHODS

2.1 Chemicals and reagents

Authentic standards of PNSs (PPD-type ginsenoside Rb1, Rb2 and Rd, PPT-type ginsenoside Re, Rf, Rg1 and notoginsenoside R1) and Panax notoginseng extract (PNE) were purchased from Department of Natural Medicinal Chemistry in Jilin University (Jilin, China). The purity of these standards was higher than 98.0 %, and the structures of these PNSs are shown in Fig. S1. TNBS, streptomycin, and neomycin sulfate were purchased from Sigma-Aldrich (St. Louis, MO). Bacteria genomic DNA extraction kit was purchased from Takara Bio (Kyoto, Japan). SYBR Green Supermix was purchased from Bio-RAD (Hercules, CA). The β-glucosidase and β-xylosidase activity assay kits were purchased from Comin Biotech (Suzhou, China). HPLC-grade acetonitrile and methanol were purchased from Fisher Scientific Inc. (Fair Lawn, USA). Deionized water was purified using a Milli-Q Ultrapure water system with the water outlet operating at 18.2 MΩ (Millipore, Bedford, USA). Other chemicals and solvents were all of analytical grade.

2.2 Animals and experimental design

The present study was approved by the Ethical Committee of Animal Experiments of China Pharmaceutical University. Healthy Sprague-Dawley rats (220 ±10 g) were provided by Shanghai Super-B & K Laboratory Animal (Shanghai, China). All animals were kept in an environmentally controlled breeding room under controlled temperature (20 ~ 24°C) and relative humidity (40 ~ 70%) with a 12-h light/dark cycle. The animals were acclimated for 5 days before use. Standard diet and water were provided to the rats ad libitum.

The TNBS-challenged rats were prepared as follows: SD rats were fasted overnight and then anesthetized using halothane. Under anesthesia, rats were administered 8 mg/kg of TNBS dissolved in 50% ethanol (v/v) by inserting a teflon cannula into the anus 8 cm. During and after

TNBS administration, the rats were kept in a head-down position until they recovered from anesthesia. For the preparation of pseudo-germ-free rats, antibiotic cocktail was prepared by dissolving neomycin sulfate and streptomycin in water, and SD rats were orally administered the antibiotic cocktail (100 mg/kg per each antibiotic) twice a day for 6 days. The experiments were performed 2 days later after the final administration.

For the metabolism studies, the rats were divided into 3 groups: 4 conventional rats in group A, 4 TNBS-challenged rats in group B, and 4 pseudo GF rats in group C, respectively. All the rats were fasted overnight with free access to water before sacrificed by cervical dislocation under ether anesthesia. Fresh fecal in ileocecal valve were collected sterilely and homogenized with 3-fold volume of preservation solution (1.8g of sodium chloride dissolved in 80ml of deionized water and 20 ml of glycerin). The sediments were removed by filtration through three pieces of gauze and the suspension was stored in -80 ℃ freezer until required.

2.3 Gut microbe gene sequencing

2.3.1 DNA extraction and PCR amplification .

Total genome DNA from rat intestinal microbiota (n=4 for each group) was extracted by hexadecyl trimethyl ammonium bromide. DNA concentration and purity was monitored on 1% agarose gels. According to the concentration, DNA was diluted to 1 ng/μl using sterile water. 16S rRNA genes of distinct regions (16SV4/16SV3/16SV3-V4/16SV4-V5) were amplified using specific primer (341F: CCTAYGGGRBGCASCAG, 806R: GGACTACNNGGGTATCTAAT) with the barcode (Jia et al. 2016). All PCR reactions were performed in a 30 μl volume containing 15 μl of Phusion DNA Polymerase, 0.5 μl of each primer (10 μM) and 1 μl of DNA template. Thermal cycling consisted of initial denaturation at 98 ℃ for 1 min, followed by 30 cycles of denaturation at 98 ℃ for 10 s, annealing at 50 ℃ for 30 s, and elongation at 72 ℃ for 30 s. Each PCR reaction was performed with Phusion® High-Fidelity PCR Master Mix (New England Biolabs). The PCR products were mixed with same volume of 2 × loading buffer and operated electrophoresis on 2% agarose gel (containing SYB green) for detection. Samples with bright main strip between 400 and 450 bp were chosen and mixed in equidensity ratios. Then, mixture PCR products were purified with Qiagen Gel Extraction Kit (Qiagen, Valencia, CA).

2.3.2 MiSeq sequencing of 16S rRNA gene amplicons.

The 16S rRNA gene amplicons were used to determine the diversity and structure comparisons of the bacterial species in rat intestinal microbiota using Illumina MiSeq sequencing at Novogene Bioinformatics Technology Co., Ltd, Tianjin, China. Sequencing libraries were generated using TruSeq ® DNA PCR-Free Sample Preparation Kit (Illumina, CA, USA) following manufacturer's recommendations and index codes were added. The library quality was assessed on the Qubit @ 2.0 Fluorometer (Thermo Scientific, Waltham, MA) and Agilent Bioanalyzer 2100 system (Agilent Technologies, Palo Alto, Calif.). At last, the library was sequenced on an Illumina HiSeq 2500 platform (Illumina, CA, USA) and 250 bp paired-end reads were generated.

2.3.3 Data analysis

Paired-end reads was assigned to samples based on their unique barcode and truncated by cutting off the barcode and primer sequence. Paired-end reads were merged using FLASH v1.2.7 (http://ccb.jhu.edu/software/FLASH/) based on overlapping regions within paired-end reads (Magoč, et al. 2011), and quality filtering on the raw tags were performed under specific filtering conditions to obtain the high-quality clean tags according to the QIIME (V1.7.0, http://qiime.org/index.html) quality control process (Caporaso et al. 2010). Tags were compared with the reference database (Gold database) using UCHIME lgorithm to detect chimera sequences, and then the chimera sequences were removed.

Sequences analysis was performed using Uparse software (Uparse v7.0.1001, http://drive5.com/uparse/). Sequences with ≥ 97 % similarity were assigned to the same Operational Taxonomic Units (OTUs). Representative sequence for each OTU was screened for further annotation. For each representative sequence, the Green Gene Database was used based on RDP classifier (Version 2.2, https://sourceforge.net/projects/rdp-classifier/) algorithmto annotate taxonomic information. OTUs abundance information was normalized using a standard of sequence number corresponding to the sample with the least sequences. Subsequent analysis of alpha diversity and beta diversity were all performed basing on this output normalized data.

2.4 Incubation of PNS monomer and PNE with intestinal microbiota

Intestinal microbiota suspension was thawed in 37 ℃ water bath and cultured with 4-fold

volume of Poly Peptone Yeast Extract medium (Invitrogen, Carlsbad, CA) in an anaerobic incubator at 37 ℃. The air in anaerobic incubator had been replaced with a gas mixture (5% H_2, 10% CO_2, and 85% N_2). After incubation for 12 h, PNS monomers (20.0 μg/ml) or PNE (200.0 μg/ml) were added to the incubation system. The incubated mixture was then extracted using n-butanol after incubating for 0.5, 1, 2 and 4 h, respectively. The extract was evaporated, and the residue was reconstituted in 0.2 ml of methanol and analyzed by LC-triple-TOF/MS.

2.5 Qualitative and quantitative analysis of metabolites based on LC-triple-TOF/MS.

A hybrid quadrupole time-of-flight tandem mass spectrometer was coupled with a Shimadzu Prominence HPLC system (AB SCIEXTriple TOF® 5600 LC-triple-TOF/MS, Foster City, CA), consisting of a LC-30A binary pump, a CTO-30AC column oven and a SIL-30AC autosampler. Chromatographic separation was achieved on C18 reversed phase LC column (Phenomenex Luna, 5 μm particles, 2.1 mm * 150 mm). The mobile phase (solvent A) was H_2O containing 0.02% acetic acid (v/v), and the organic phase (solvent B) was acetonitrile. A 45 min binary gradient elution (delivered at 0.2 ml/min) was performed for the separation: an isocratic elution of 15% solvent B for the initial 5 min, followed by a linear gradient to 45% solvent B in 20 min (elapsed time 25 min); then followed by another linear gradient to 90% solvent B in 10 min (elapsed time 35 min); after holding 90% B for the next 5 min, the column was returned to its starting conditions till the end of the gradient program at 41 min for column re-equilibration. LC-triple-TOF/MS, a hybrid triple quadrupole time-of-flight mass spectrometer equipped with a Turbo V source, was used to analyze the samples in negative ionization mode. The optimized MS conditions were as follows: ionspray voltage, 4.5 kV; declustering potential (DP), 100 V; the turbo spray temperature, 500℃; nebulizer gas (Gas 1), 50 psi; heater gas (Gas 2), 60 psi; curtain gas, 30 psi. Nitrogen was kept as nebulizer and auxiliary gas. The triple-TOF/MS scan was operated with the mass range of m/z 200 ~ 1250 Da. A typical information dependent acquisition (IDA) was used to carry MS/MS experiment. For IDA, product ion scan was acquired in 250 ms if precursor ions exceeded a threshold of 300 counts per second. A sweeping collision energy setting at 30 ± 15 eV was applied for collision-induced dissociation. Collision gas was set at 10 psi. Continuous recalibration was carried out every 6 h by EasyMass Accuracy device.

2.6 Assay of Glycosidase Activities

The pellets of bacteria were collected as mentioned above. Then 500 μl of extraction solution was added, and the bacteria were crashed by ultrasoincation. The activities of β-glucosidase and β-xylosidase were determined by the glycosidase assay kits according to the manufacturer's protocol. Protein concentrations were determined by the BCA protein assay kit (Jian Cheng Biotech, Nanjing, China).

2.7 Data Analysis

Each experiment was performed in triplicate with at least 4 independent samples. Data sets were evaluated using t-test or One-Way Analysis of Variance (ANOVA) followed by Tukey's post hoc test, and expressed as mean ± SD. Statistically significant difference was set at $P < 0.05$.

3. RESULTS

3.1 Bacterial community structures of the conventional, TNBS-challenged and pseudo GF rat intestinal microflora

In the present study, we characterized the intestinal bacterial community of the conventional, TNBS-challenged and pseudo GF rats via 16S rRNA amplicon Illumina sequencing as described in materials and methods sections above. The taxon abundance of each specimen was generated into phylum, class, order, family, and genera levels. Firstly, a total number of 58228, 52609 and 62817 of 16S rRNA valid sequence reads were obtained from conventional, TNBS-challenged and pseudo GF rat intestinal flora, respectively, which indicates that the 16S rRNA gene sequence database was abundant enough to capture most of the microbial diversity information (Fig. S2).

To clearly visualize the difference in the bacterial community of the conventional, TNBS-challenged and pseudo GF rats (n=4), stacked column chart of the dominant bacterial genera were constructed based on the top 10 relative abundance of gut microbe in each group using the QIIME toolkit (Fig. 1). As shown in Fig. 1A, Firmicutes, Bacteroidetes and Proteobacteria were identified as the major bacterial phylum of the rat bacterial community. Based on relative abundance, Proteobacteria in the pseudo GF rat intestinal flora was much lower than that in the conventional and TNBS-challenged rats. Tenericutes has higher relative abundance in

conventional rats compared with other model rats, and the relative abundance of Fusobacteria in TNBS-challenged rats was much higher than that in the conventional and pseudo GF rats. The bacterial diversity and relative abundance at the family level are presented in Fig. 1B. Obviously, microbial communities in the conventional, TNBS-challenged and pseudo GF rats mainly consist of Bacteroidia and Clostridia. Epsilonproteobacteria had higher relative abundance in conventional rats compared with other model rats, and relative abundance of Erysipelotrichia (over 25%) in the pseudo GF rats was much higher than that in the conventional and TNBS-challenged rats. At the order level, Bacteroidales and Clostridiales had higher relative abundance compared with other bacteria. In the control group, Campylobacterales in conventional rats had much higher relative abundance than that in the TNBS-challenged and pseudo GF rats. In pseudo GF rats, the relative abundance of Erysipelotrichales was much higher than that of the other two groups (Fig. 1C). The bacterial diversity and relative abundance of all rat intestinal flora in the different family are presented in Fig. 1D. The results showed that conventional rats had a gut microbe community dominated by Lachnospiraceae, Bacteroidales_S24-7_group, Helicobacteraceae and Ruminococcaceae. After treating with TNBS, the relative abundance of Bacteroidaceae, Bacteroidales_S24-7_group, Helicobacteraceae was significantly decreased. In addition, pseudo GF rats showed a substantial growth of Bacteroidales and Erysipelotrichaceae accompanied by significant decreasing of Bacteroidales_S24-7_group, Helicobacteraceae and Ruminococcaceae compared with the conventional rats. At the genus level, great difference was found among the conventional, TNBS-challenged and pseudo GF rat intestinal bacterial community. In the conventional rats, Helicobacter had much higher relative abundance than that in TNBS-challenged and pseudo GF rats. Meanwhile, Bacteroides, Erysipelatoclostridium and Blautia were identified as the major bacterial taxa of the intestinal flora of pseudo GF rats, and Bacteroides was the most abundant bacterium with an average relative abundance of over 50%. In the TNBS-challenged rats, Lachnospiraceae_NK4A136_group was identified as the major bacterial taxa with an average relative abundance of over 20%.

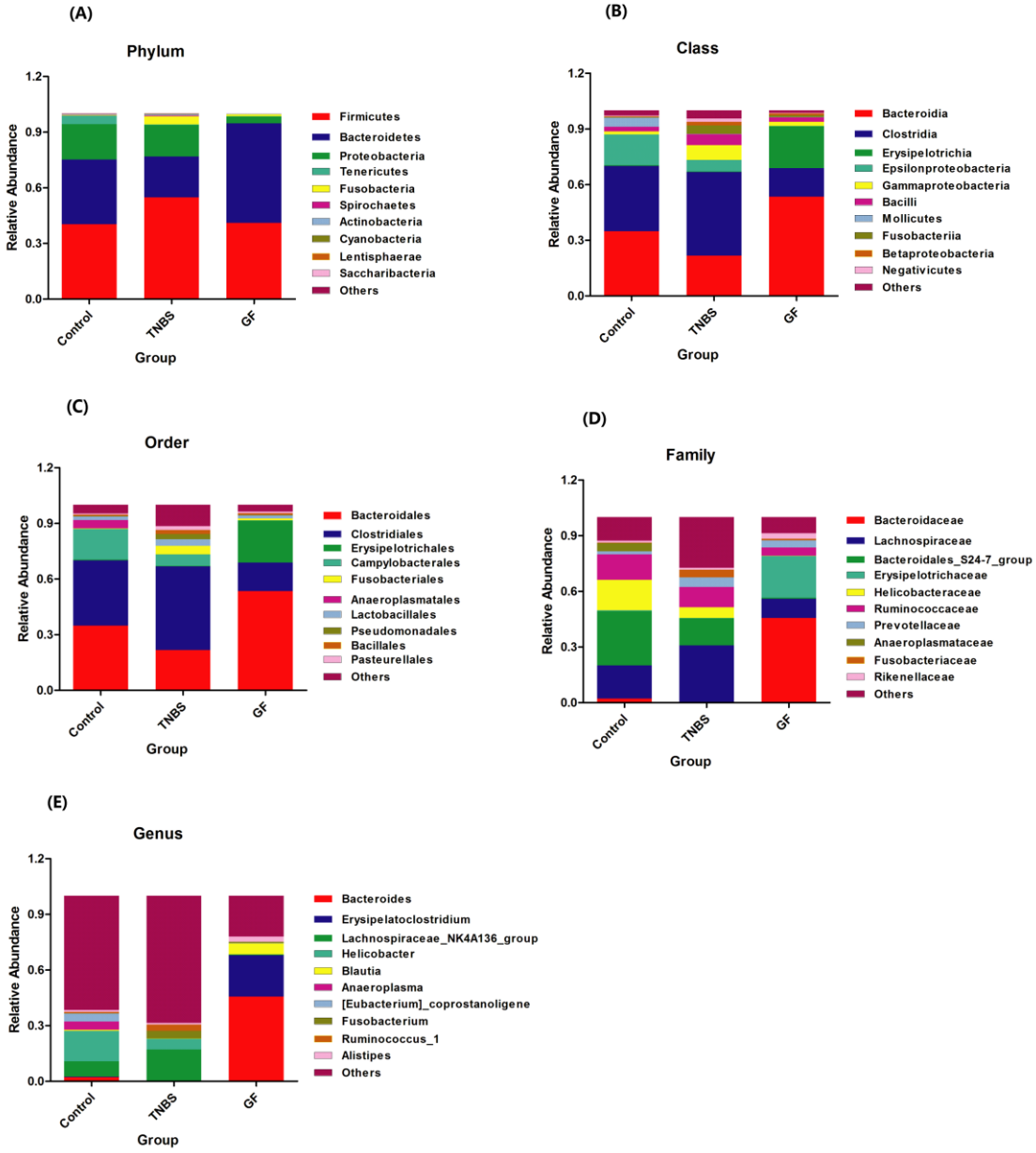

Fig. 1 Relative abundance of the dominant bacterial in the conventional, TNBS-challenged and pseudo GF rat intestinal microflora at phylum, class, order, family and genus levels. (A) relative abundance of the dominant bacterial at phylum level, (B) relative abundance of the dominant bacterial at class level, (C) relative abundance of the dominant bacterial at order level, (D) relative abundance of the dominant bacterial at family level, (E) relative abundance of the dominant bacterial at genus level.

Subsequently, the shifts of the bacterial community compositions were further corroborated by clustering of the top 35 abundance of gut microbe at genus level corresponding to different rat groups and drawing the taxa heatmap. As shown in Fig. 2, Ruminiclostridium_9, Coprococcus_1 and Helicobacter, which belong to proteobacteria phylum, had the highest level in conventional rats. Alistipes, Paraprevotella and Bacteroides, which belong to Bacteroidetes phylum, had the

highest level in pseudo GF rats. Thus, composition of intestinal flora among the conventional, TNBS-challenged and pseudo GF rats was significantly different.

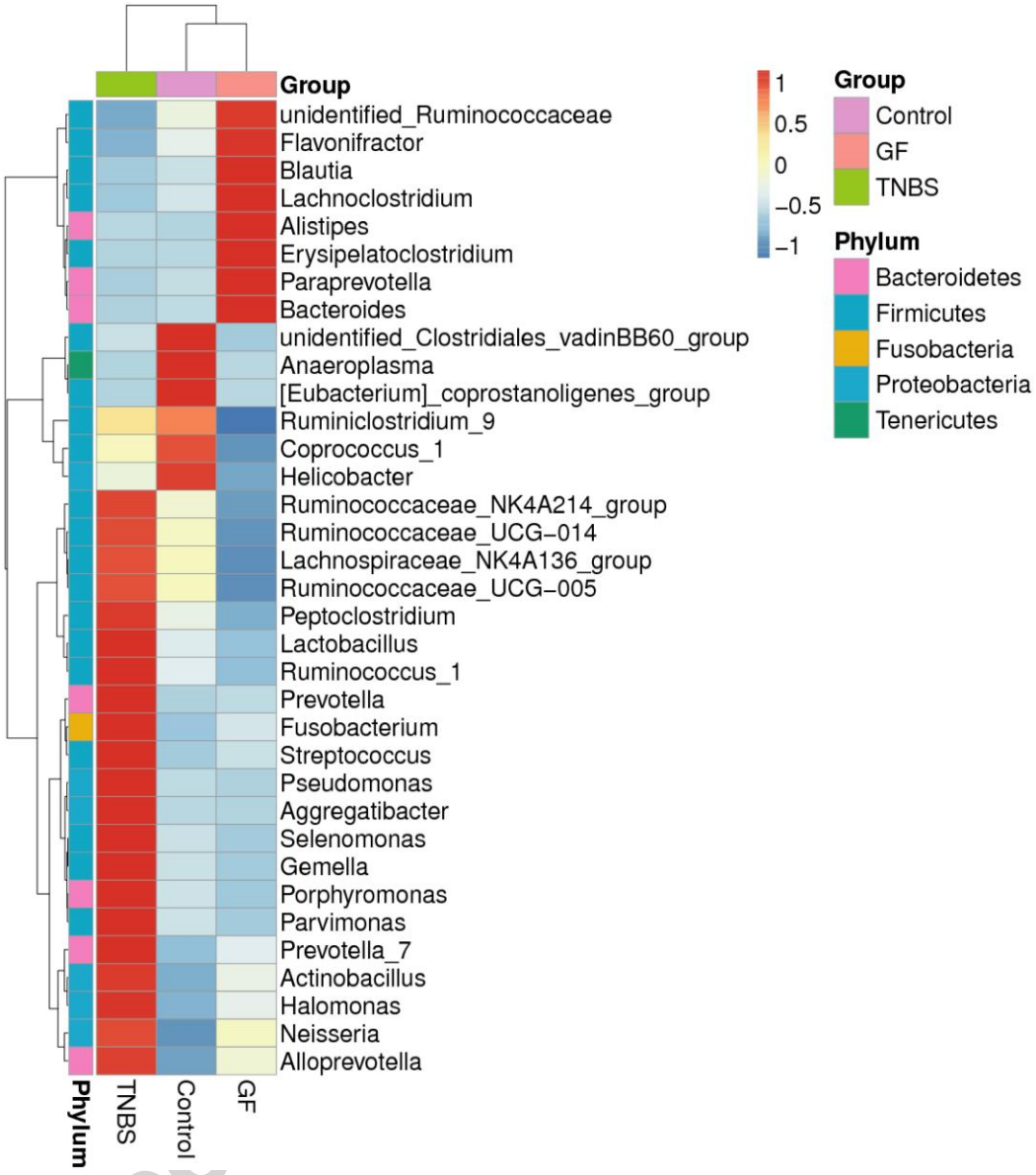

Fig. 2 Hierarchically clustered heat map analysis of the top 35 abundance of gut microbe at the genus level in conventional, TNBS-challenged and pseudo GF rat intestinal microflora. The relative percentages (%) of the bacterial families are indicated by varying colour intensities according to the legend at the top of the figure.

Table 1 The information about formula, retention time and product ions of the metabolites of protopanaxadiol-type PNSs (ginsenoside Rb1, Rb2 and Rd) identified in conventional, TNBS-challenged and pseudo germ-free rat intestinal microbiota.

Metabolite	Formula	Reaction	R.T(min)	M1	M2	Control	TNBS	GF
Rb1-M1	C48H82O18	Rb1-Glu	9.96	945.5492	783.4945 621.4360 323.0908 179.0559	√	√	
Rb1-M2	C42H70O12	Rb1-2Glu-H2O	10.62	765.4853	743.4000 603.4366 423.2821 363.2174 161.0472	√	√	
Rb1-M3	C48H82O18	Rb1-Glu	10.88	945.5477	783.4908 621.4375 459.3858 161.0462	√	√	√
Rb1-M4	C42H72O13	Rb1-2Glu	12.21	783.4931	621.4364 391.2854 323.1016 161.0470	√	√	√
Rb1-M5	C36H62O8	Rb1-3Glu	14.32	621.4359	505.2457 471.2816 315.1910 279.1548	√	√	√
Rb2-M1	C42H70O12	Rb2-Glu-Xyl-H2O	10.31	765.4836	721.4194 603.4237 574.3002 423.2329	√	√	
Rb2-M2	C48H82O18	Rb2-Xyl	10.32	945.5423	901.5579 783.4899 621.4349 493.3287	√	√	√
Rb2-M3	C48H82O18	Rb2-Xyl	10.88	945.5424	783.4937 621.4382 459.3837 161.0453	√	√	√
Rb2-M4	C47H80O17	Rb2-Glu	11.64	915.5388	783.4916 621.4404 507.2860 311.0996 293.0876 149.0455	√	√	√
Rb2-M5	C42H72O13	Rb2-Glu-Xyl	12.18	783.4936	621.4361 391.2853 101.0258	√	√	√
Rb2-M6	C36H62O8	Rb2-2Glu-Xyl	12.32	621.4388	577.3528 393.2438 215.1650 167.0438	√	√	√
Rd-M1	C48H84O19	Rd-H_2O	4.74	963.5541	919.5251 875.4937	√	√	√
Rd-M2	C42H68O14	Rd-Glu+O-4H	7.32	795.4218	777.4133 751.4389 503.2012	√	√	√
Rd-M3	C48H84O20	Rd+H2O+O	7.70	979.553	817.4988 799.4835	√	√	√
Rd-M4	C41H68O13	Rd-Glu-CH2-2H	11.3	767.4642	687.4252 467.1767 241.1152 195.0745	√	√	√
Rd-M5	C35H58O8	Rd-2Glu-CH2-2H	12.21	605.4087	562.3616 527.2806 421.2442 227.1370 209.0918	√	√	
Rd-M6	C42H72O13	Rd-Glu	12.38	783.5798	781.1163 621.4364 391.2852 161.0439	√	√	√

3.2 Qualitative analysis of the metabolites of protopanaxadiol-type PNSs (PPDs) in microbiota from conventional, TNBS-challenged and pseudo GF rats

To obtain the metabolite profiles of PPDs in rat intestinal microbiota, three PPD-type standards (ginsenoside Rb1, Rb2 and Rd) were incubated with microbiota collected from conventional, TNBS-challenged and pseudo GF rats, respectively, and the metabolite profiles were obtained by LC–triple-TOF/MS in the negative ion mode. Then, the Metabolite Pilot™ software was used to screen metabolites via comparing the empirical MS (MS^E) LC–MS data of the sample and control automatically, and the structures of the metabolites were then tentatively deduced by interpretation of their accurate MS^1 and MS^2 data. The information about formula, retention time and product ions of the metabolites identified in conventional, TNBS-challenged and pseudo GF rat intestinal microbiota is list in Table 1.

For ginsenoside Rb1 ($C_{54}H_{92}O_{23}$, m/z 1107.5951), 5 main metabolites (Rb1-M1~ Rb1-M5) were detected in conventional and TNBS-challenged groups, and only 3 main metabolites (Rb1-M3~ Rb1-M5) were found in the pseudo GF group. Rb1-M1 and Rb1-M3 were deduced as the deglycosylated metabolites of ginsenoside Rb1 according to their accurate MS^1 and MS^2 information. The metabolite Rb1-M2, eluted at 10.62 min, was calculated as $C_{42}H_{70}O_{12}$ by the Formula Finder software according to the accurate mass at m/z 765.4853 ($[M-H]^-$). The spectra of MS^2 showed 5 major product ions at 743.4000, 603.4366, 423.2821, 363.2174 and 161.0472. According to those characteristic product ions, Rb1-M2 could be identified as the deglucosylation & dehydration product of ginsenoside Rb1. Similarly, Rb1-M4 and Rb1-M5 were identified as the metabolites resulting from successive loss of glucosyl groups from ginsenoside Rb1 via comparing the accurate MS^1 and MS^2 information with their parent compound Rb1.

For ginsenoside Rb2 ($C_{53}H_{90}O_{22}$, m/z 1077.5845), 6 main metabolites (Rb2-M1~ Rb2-M6) were detected in conventional and TNBS-challenged groups. Except for the Rb2-M1, the other 5 main metabolites (Rb2-M2~ Rb2-M6) were identified in the pseudo GF rat fecal microbiota incubation system. Rb2-M1, showed m/z 765.4836 ($[M - H]^-$), was calculated as $C_{42}H_{70}O_{12}$. By comparing the elemental composition and characteristic product ions with that of parent compound, Rb2-M1 was identified as a deglucosylated & dexylosylated & dehydrated product of

ginsenoside Rb2. Likewise, Rb2-M2 and Rb2-M3 were identified as the metabolites resulting from successive loss of xylose from ginsenoside Rb2. The metabolite Rb2-M4, eluted at 11.64 min, was calculated as $C_{47}H_{80}O_{17}$ based on their HRMS data. According to its fragmental patterns inferred from the characteristic product ions, Rb2-M4 was identified as the metabolite resulting from the loss of glucose. For Rb2-M5, the observed parent ion ($[M-H]^-$) was at m/z 783.4936, which was 132 Da less than that of Rb2-M4. Thus, Rb2-M5 was formed by the successive loss of glucose and xylose from ginsenoside Rb2. Similarly, the observed parent ion ($[M-H]^-$) of Rb2-M6 was at m/z 621.4388 which was 162 Da less than that of Rb2-M5, and the parent ion of Rb2-M6 was same with dominant fragmental ion of Rb2-M5, which suggesting that Rb2-M6 was formed by loss of glucose from ginsenoside Rb2-M5.

For ginsenoside Rd ($C_{48}H_{82}O_{18}$, m/z 945.5423), 6 main metabolites (Rd-M1~ Rd-M6) were detected in conventional and TNBS-challenged rat intestinal microbiota. Besides Except for Rd-M5, the other 5 main metabolites (Rd-M1~ Rd-M4, Rd-M6) were identified in the pseudo GF rat intestinal microbiota. Rd-M1, eluted at 4.74 min, was determined to be $C_{48}H_{84}O_{19}$ based on its accurate MS^1 data. By comparing the formula with that of parent compound, Rd-M1 was identified as the dehydrated product of ginsenoside Rd. Rd-M2, showed $[M-H]^-$ at m/z 795.4218, which indicated that its molecular formula was calculated as $C_{42}H_{68}O_{14}$. According to its accurate MS^1 and MS^2 data, Rd-M2 was identified as the deglucosylation & oxidization & dehydrogenation product of ginsenoside Rd. By comparing the formula ($C_{48}H_{84}O_{20}$) with that of Rd-M1, Rd-M3 was identified as an oxidized product of Rd-M1. Rd-M4 showed $[M-H]^-$ at m/z 767.4642, and its molecular formula was calculated as $C_{41}H_{68}O_{13}$. Besides, 4 characteristic fragment ions at m/z 687.4252, 467.1767, 241.1152 and 195.0745 appeared in the MS^2 spectrum, which indicating that the Rd-M4 was the deglucosylated & demethylated & dehydrogenated product of ginsenoside Rd. By analogy, Rd-M5 was deduced as the deglucosylated product of Rd-M4, and Rd-M6 was identified as deglucosylated product of ginsenoside Rd.

Table 2 The information about formula, retention time and product ions of the metabolites of protopanaxatriol-type PNSs (ginsenoside Re, Rf, Rg1, Rg2 and notoginsenoside R1) identified in conventional, TNBS-challenged and pseudo germ-free rat intestinal microbiota.

Metabolite	Formula	Reaction	R.T.	M1	M2	Control	TNBS	Antibiotics
Re-M1	C48H84O19	Re+H_2O	6.26	963.5529	919.5336; 875.4964; 481.2309	√	√	√
Re-M2	C42H72O13	Re-Glu	8.10	783.4922	765.4011; 637.4352; 621.3199; 545.3866; 113.0214	√	√	√
Re-M3	C36H62O9	Re-Glu-Rha	9.34	637.4338	593.3664; 475.3249; 239.1180; 227.1384	√	√	√
Re-M4	C42H72O14	Re-Rha	8.74	799.4025	781.4136; 755.3229	√	√	√
Re-M5	C30H52O4	Re-2Glu-Rha	13.2	475.3799	333.1274 261.1238 113.0701	√	√	√
Re-M6	C48H78O18	Re-4H	7.68	941.5185	923.4481 897.4416	√	√	√
Re-M7	C42H68O14	Re-Glu+O-4H	7.20	795.4524	680.3883 552.3205 456.2255 312.2069 242.1277	√	√	
Rf-M1	C36H62O9	Rf-Glu	11.27	637.4351	593.3673 475.3799 161.0447	√	√	
Rf-M2	C36H62O9	Rf-Glu	10.82	637.4348	475.3780 457.3586 391.2695 161.0458	√	√	√
Rf-M3	C30H52O4	Rf-2Glu	12.06	475.3783	431.3662 393.2808	√	√	√
Rf-M4	C41H70O13	Rf-CH2O	10.39	769.4748	637.4339 475.3795 161.0458 113.0227	√	√	
Rg1-M1	C36H60O8	Rg1-Glu-H2O	11.20	619.2787	575.3067 502.3215 361.1585 209.1256	√	√	√
Rg1-M2	C36H62O9	Rg1-Glu	10.76	637.4325	475.3715 391.2970 297.1111 161.0447	√	√	√
Rg1-M3	C30H52O4	Rg1-2Glu	12.07	475.3793	413.3100 393.2318	√	√	√
R1-M1	C30H52O4	R1-2Glu-Xyl	13.08	475.3798	391.2825	√	√	√
R1-M2	C41H70O13	R1-Glu	7.43	769.4782	637.4351 475.3785 161.0444	√	√	√
R1-M3	C36H62O9	R1-Glu-Xyl	10.89	637.4355	575.3744 475.3780 339.2082 227.1510	√	√	√
R1-M4	C36H62O9	R1-Glu-Xyl	11.31	637.4355	475.3812 161.0445	√	√	
R1-M5	C42H72O14	R1-Xyl	7.61	799.4912	755.4204 637.4353 635.2785 475.3857	√	√	√
R1-M6	C42H72O14	R1-Xyl	8.04	799.4912	637.4363 475.3801 161.0453	√	√	√
R1-M7	C47H78O18	R1-2H	7.69	929.5191	797.4743 635.4191 473.3641 179.0532	√	√	√
R1-M8	C41H66O13	R1-Glu-4H	6.61	765.4570	721.4982 659.3035 591.3051 427.7943	√	√	√
R1-M9	C42H68O14	R1-Xyl-4H	7.87	795.4366	635.3548 475.3747	√	√	√
R1-M10	C47H76O19	R1+O	8.32	943.4942	763.4293 335.0206 227.1384	√	√	√
R1-M11	C46H76O19	R1-CH3+O	7.42	931.5357	799.4910 637.4357 475.3805 161.0446	√	√	√

3.3 Qualitative analysis of the metabolites of protopanaxatriol-type PNSs (PPTs) in microbiota from conventional, TNBS-challenged and pseudo GF rats

To obtain the metabolite profiles of PPTs in rat intestinal microbiota, four PPT-type standards (ginsenoside Re, Rf, Rg1 and notoginsenoside R1) were incubated with conventional, TNBS-challenged and pseudo GF rat intestinal microbiota, respectively. The information about formula, retention time and product ions of the metabolites of ginsenoside Rb1, Rb2, Rd and notoginsenoside R1 is list in Table 2.

For ginsenoside Re ($C_{48}H_{82}O_{18}$, m/z 945.5423), 7 main metabolites (Re-M1~ Re-M7) were detected in conventional and TNBS-challenged rat intestinal microbiota, and 6 main metabolites (Re-M1~ Re-M6) were identified in the pseudo GF group. Re-M1, eluted at 6.26 min, was determined to be $C_{48}H_{84}O_{19}$ based on their accurate MS^1 data. By comparing the formula with that of parent compound, Re-M1 was identified as the dehydrated product of ginsenoside Re. Re-M2, eluted at 8.10 min, showed m/z at 783.4922 ($[M-H]^-$), which suggesting that its molecular formula was $C_{42}H_{72}O_{13}$. Five characteristic fragment ions at m/z 765.4011, 637.4352, 621.3199, 545.3866 and 113.0214 indicated that the Re-M2 was the deglucosylated product of ginsenoside Re. Re-M3 showed $[M-H]^-$ at m/z 637.4338 and its molecular formula was calculated as $C_{36}H_{62}O_9$. Besides, fragment ions at m/z 593.3664, 475.3249, 239.1180 and 227.1384 suggested that the Re-M3 was the deglucosylated & derhamnosylated product of ginsenoside Re. By analogy, Re-M4 was deduced as the derhamnosylated product of ginsenoside Re, and Re-M5 was found to be formed by loss of two glucose molecules and one rhamnose from ginsenoside Re. Re-M6, eluted at 7.68 min, showed m/z at 941.5185 ($[M-H]^-$), suggesting that its molecular formula was $C_{48}H_{78}O_{18}$. By comparing the formula with that of parent compound, Re-M6 was identified as a dehydrogenated product of ginsenoside Re. Re-M7 was eluted at 7.20 min with quasi-molecular ion of m/z 795.4424, which suggested that Re-M7 was an oxidative and dehydrogenated product of Re-M2.

For ginsenoside Rf ($C_{42}H_{72}O_{14}$, m/z 799.4844), 4 main metabolites (Rf-M1~ Rf-M4) were detected in conventional and TNBS-challenged rat intestinal microbiota, and 2 main metabolites (Rf-M2 and Rf-M3) were identified in the pseudo GF rat intestinal microbiota incubation system. Rf-M1 and Rf-M2 were eluted at 11.27 and 10.82 min with the quasi-molecular ions of m/z

637.43 ($C_{36}H_{62}O_9$). Based on their fragmental pathways, Rf-M1 and Rf-M2 were tentatively identified as the deglucosylated products of ginsenoside Rf. Besides, Rf-M3 was identified as deglucosylated product of Rf-M1 after comparing the formula with that of Rf-M1. The quasi-molecular ion of m/z 769.4748 (Rf-M4, $C_{41}H_{70}O_{13}$), eluted at 10.39 min, was 30 Da less than the quasi-molecular ion of ginsenoside Rf, which suggested that Rf-M4 was formed by loss of CH_2O from ginsenoside Rf.

For ginsenoside Rg1 ($C_{42}H_{72}O_{14}$, m/z 799.4844), 3 main metabolites (Rg1-M1~ Rg1-M3) were detected in rat fecal microbiota. Rg1-M1, eluted at 11.20 min, could produce distinctive product ions at m/z 575.3067, 502.3215, 361.1585 and 209.1256, suggesting that Rg1-M1 was formed by loss of glucose and H_2O from ginsenoside Rg1. Similarly, Rg1-M2 was found to be formed by loss of glucose from the parent compound. Besides, Rg1-M3 was concluded as the deglucosylated product of Rg1-M2 by comparing its elemental composition and fragmental pathway with those of Rg1-M2.

For notoginsenoside R1 ($C_{47}H_{82}O_{18}$, m/z 931.5266), 11 main metabolites (R1-M1~ R1-M11) were detected in conventional and TNBS-challenged groups, and 10 main metabolites (R1-M1~ R1-M3, R1-M5~ R1-M11) were identified in the pseudo GF rat intestinal microbiota incubation system. R1-M1 (m/z 475.3798), eluted at 13.08 min, was found to be formed by loss of 2 glucose molecules and 1 xylose molecule from the parent compound. R1-M2, eluted at 7.43 min with the quasi-molecular ion of m/z 769.4782 ($C_{41}H_{70}O_{13}$), was found to be formed by loss of glucose from notoginsenoside R1. R1-M3 and R1-M4, showed $[M-H]^-$ at m/z 637.4355, which indicated that their molecular formula was $C_{36}H_{62}O_9$. In the MS^2 spectrum, the common fragment ion at m/z 475.3812 was formed by loss of glucose. Then, R1-M3 and R1-M4 was identified as the deglucosylation & dexylosylation products of notoginsenoside R1 according to their characteristic product ions. Similarly, R1-M5 and R1-M6 was identified as the dexylosylation products of notoginsenoside R1. The quasi-molecular ion of m/z 929.5191 (R1-M7, $C_{47}H_{78}O_{18}$), eluted at 7.69 min, was 2 Da less than the quasi-molecular ion of R1, which suggested that R1-M7 was formed by loss of hydrogen from R1. R1-M8 was eluted at 6.61 min with quasi-molecular ion of m/z 765.4570, which suggested that R1-M8 was formed by loss of glucose molecule and hydrogen

from notoginsenoside R1. R1-M9, eluted at 7.87 min with quasi-molecular ion of m/z 795.4366, was found to be formed by loss of xylcose molecule and hydrogen from R1. The metabolite R1-M10, eluted at 8.32 min, showed mass-to-charge ratios of m/z 943.4942 ($[M - H]^-$), suggesting that its molecular formula was $C_{47}H_{76}O_{19}$. By comparing the formula with that of parent compound, R1-M10 was identified as an oxidized product of parent compound. By comparing the formula with that of R1-M10, R1-M11 was identified as a demethyl product of R1-M10.

3.4 Relative quantitative analysis of the metabolites for PNSs in conventional, TNBS-challenged and pseudo GF rat intestinal microbiota

To further investigate the capability of enzyme in gut microflora on catalyzing the metabolism of PNSs, the relative exposure of metabolites in conventional, TNBS-challenged and pseudo GF rat intestinal microbiota was calculated by comparing the peak area generated by LC-triple-TOF/MS.

For the ginsenoside Rb1, 5 main metabolites (Rb1-M1 ~ Rb1-M5) were detected in conventional and TNBS-challenged rat intestinal microbiota. As shown in Fig. 3A, the relative exposure of the metabolite Rb1-M1, Rb1-M3 and Rb1-M5 in TNBS-challenged rat intestinal microbiota was significantly lower than that in conventional group, and the metabolite Rb1-M2 and Rb1-M4 had similar exposure levels in TNBS-challenged and conventional groups. In pseudo GF group, only 3 main metabolites (Rb1-M3~ Rb1-M5) were identified, and their relative exposure levels were significantly lower than those in TNBS-challenged and conventional groups ($P < 0.01$). For ginsenoside Rb2, 6 main metabolites (Rb2-M1 ~ Rb2-M6) were detected in conventional and TNBS-challenged groups. As shown in Fig. 3B, the relative exposure of metabolite Rb2-M2, Rb2-M4 ~ Rb2-M6 in TNBS-challenged group was much lower than that in conventional group, and the metabolite Rb1-M1 and Rb1-M3 had similar exposure levels in these two groups. Besides, the relative exposure levels of the metabolites (Rb2-M2 ~ Rb2-M6) identified in the pseudo GF group were significantly lower than those in TNBS-challenged and conventional groups ($P < 0.01$). For ginsenoside Rd, the metabolites (Rd-M1~Rd-M4) had similar exposure levels in the two groups, and the relative exposure of metabolite Rd-M5 and Rd-M6 in conventional group was much higher than that in TNBS-challenged group. Besides, 5 main

metabolites (Rd-M1~ Rd-M4, Rd-M6) were identified in the pseudo GF rat intestinal microbiota incubation system. For Rd-M1, Rd-M2 and Rd-M6, their relative exposure levels were much lower than those in the conventional and TNBS-challenged groups. Unexpectedly, the relative exposure levels of Rd-M3 and Rd-M4 in pseudo GF were much higher than those in the conventional and TNBS-challenged groups (Fig. 3C).

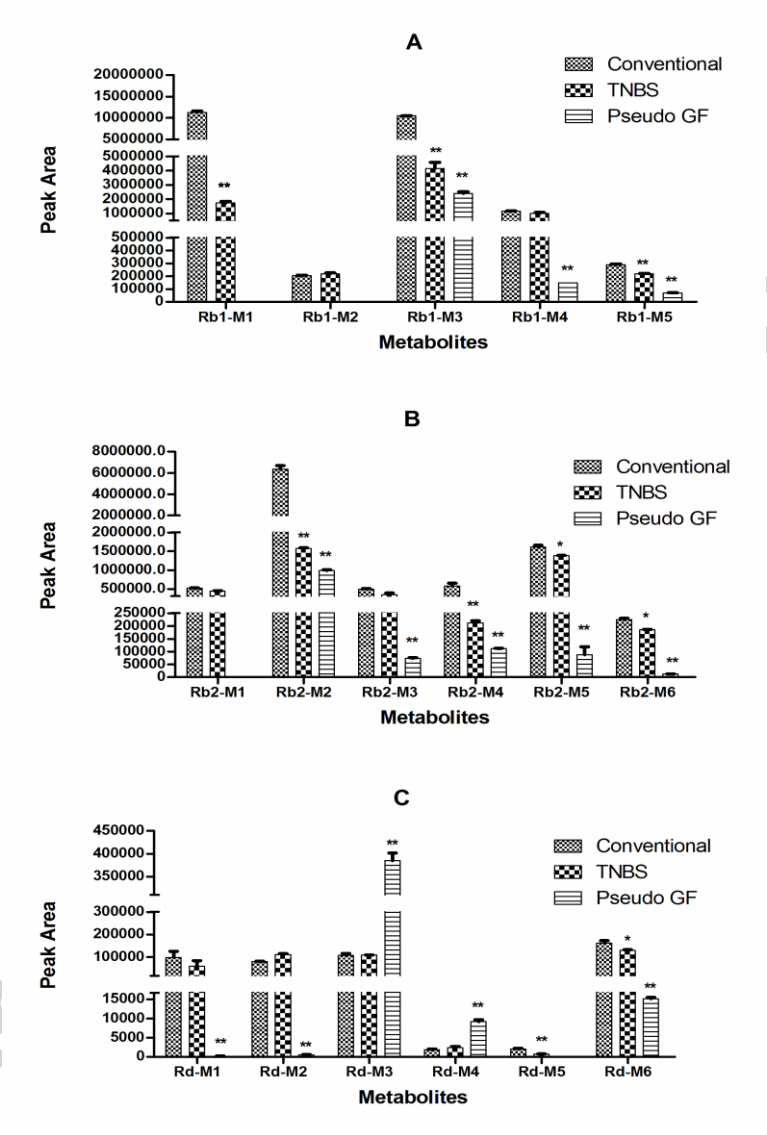

Fig. 3 The exposure levels of the metabolites of the PPD-type PNSs (ginsenoside Rb1, Rb2 and Rd) in the conventional, TNBS-challenged and pseudo GF rat intestinal microbiota. (A) the exposure levels of the metabolites of the ginsenoside Rb1, (B) the exposure levels of the metabolites of the ginsenoside Rb2, (C) the exposure levels of the metabolites of the ginsenoside Rd.

For ginsenoside Re, 7 main metabolites (Re-M1~ Re-M7) were detected in conventional and TNBS-challenged rat intestinal microbiota. As shown in Fig. 4A, the relative exposure of the metabolite Re-M2, Re-M4 and Re-M5 in TNBS-challenged group was much lower than that in conventional group, and the metabolite Re-M1, Re-M3, Re-M6 and Re-M7 had similar exposure levels in these two groups. In the pseudo GF rat intestinal microbiota incubation system, 6 main metabolites (Re-M1~ Re-M6) were identified, and the relative exposure levels of Re-M1 ~ Re-M5 were much lower than those in the conventional group. On the contrary, Re-M6 in the pseudo GF group had 3-fold higher intensity than those in the conventional and TNBS-challenged groups. For the ginsenoside Rf, 4 main metabolites (Rf-M1~ Rf-M4) were detected in conventional and TNBS-challenged groups, and the peak intensities of Rf-M1, Rf-M3 and Rf-M4 were similar in the two groups. The metabolite Rf-M2 had much higher intensity in the conventional group than that in the TNBS-challenged group, and the exposure levels of Rf-M2 in the three incubation system were quantified in the following order: conventional > pseudo GF > TNBS-challenged. The exposure level of Rf-M3 in the pseudo GF group was significantly lower than the other groups (Fig. 4B). For ginsenoside Rg1, the exposure levels of the metabolites were similar in the conventional and TNBS-challenged groups, and the peak intensities of the metabolites in the pseudo GF group was significantly lower than those in the other groups (Fig. 4C). For notoginsenoside R1, 11 main metabolites (R1-M1~ R1-M11) were detected in conventional and TNBS-challenged rat intestinal microbiota. The metabolite R1-M6 showed much higher intensity in the conventional group than that in the TNBS-challenged group, and the exposure levels of the other metabolites were similar in the conventional and TNBS-challenged groups. Except for the R1-M4, all the metabolites were identified in the pseudo GF rat intestinal microbiota incubation system. For R1-M1~ R1-M3 and R1-M6, the relative exposure levels were much lower than those in the conventional and TNBS-challenged groups. Contrarily, the relative exposure levels of the metabolite R1-M7~ R1-M9 and R1-M11 in pseudo GF were much higher than those in the other groups (Fig. 4D).

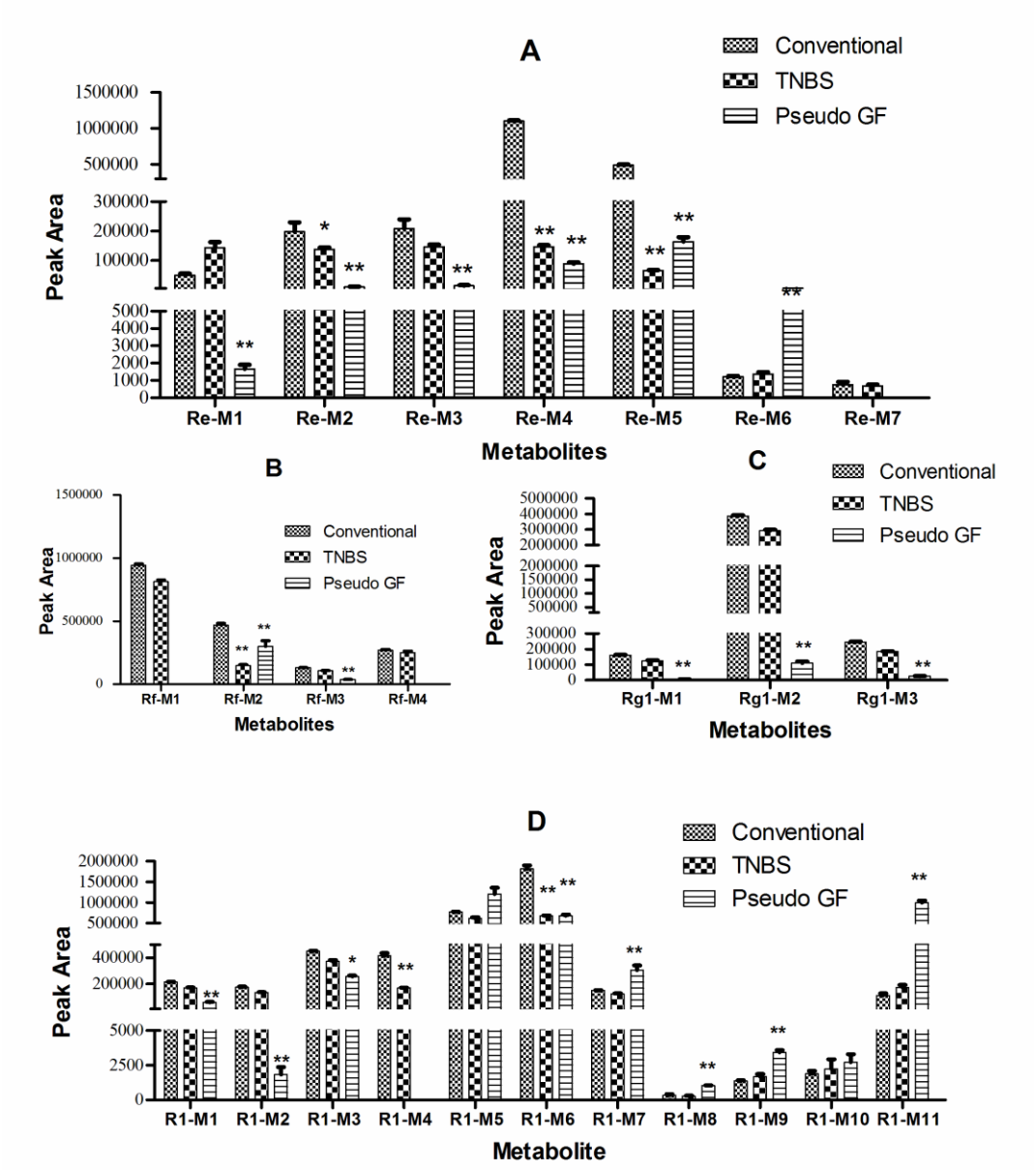

Fig. 4 The exposure levels of the metabolites of the PPT-type PNSs (ginsenoside Re, Rf, Rg1 and notoginsenoside R1) in the conventional, TNBS-challenged and Pseudo GF rat intestinal microbiota. (A) the exposure levels of the metabolites of the ginsenoside Re, (B) the exposure levels of the metabolites of the ginsenoside Rf, (C) the exposure levels of the metabolites of the ginsenoside Rg1, (D) the exposure levels of the metabolites of the notoginsenoside R1.

3.5 Qualitative and quantitative analysis of the metabolites for PNE in conventional, TNBS-challenged and pseudo GF rat intestinal microbiota

The metabolism of PNE in rat intestinal microbiota was studied from qualitative and quantitative angles based on LC-triple-TOF/MS. After comparing the constitute profiles blank intestinal microbiota with dosed intestinal microbiota, 39 metabolites were identified in the conventional and TNBS-challenged groups, and 35 metabolites were identified in the pseudo GF group based on our previous developed multiple product ions filtering (mPIF) and neutral loss filtering (NLF) techniques (Xing et al., 2015). The total ion chromatogram (TIC) of blank and dosed rat intestinal microbiota were illustrated in Fig. S3, and the information about formula, retention time and product ions of the metabolites is listed in Table S1.

In our previous studies, we built a chemicalome-metabolome matching approach (CMMA) to correlate the chemicalome with metabolome for complex compounds in herbs, and this approach was successfully used to identify metabolites for Mai-Luo-Ning and Panax notoginseng in rat excreta specimen in the past two years (Gong et al., 2012; Xing et al., 2015). Herein, the CMMA technique was applied to identify and classify the metabolites based on common and uncommon metabolic pathways. As shown in Table S1, the metabolites (M1 ~ M39) detected in rat intestinal microbiota were successfully linked to their corresponding parent compounds. Most of the metabolites were identified as the deglycosylation products. Besides, hydration, dehydration, demethylation and oxidation were deduced as the common metabolic reaction types of PNSs in rat intestinal microbiota. More importantly, the peak area generated by LC-triple-TOF/MS was used to calculate the exposure of the metabolites in the conventional, TNBS-challenged and pseudo GF rat intestinal microbiota (Table S2). The average metabolite peak area ratio of PNE in TNBS-challenged and conventional groups is shown in Fig. 5A, and the average metabolite peak area ratio of PNE in pseudo GF group and conventional group is shown in Fig. 5B. The results clearly indicated that most of the metabolites in TNBS-challenged group had similar exposure levels with those in the conventional group excluding M12, M18, M23, M28, M31, M32 and M38. In the pseudo GF group, the peak area of M5, M10, M16, M17, M18, M19, M21, M22, M26, M30, M31, M33, M36, M37 and M39, which formed by loss of glucose, xylose and rhamnose, was significantly lower than that in the conventional rats. On the contrary, the peak area of M2, M6,

M9, M12, M14, M15, M29 and M32, which were formed by oxidation, dehydrogenation, demethylation, etc, was significantly higher than that in the conventional group.

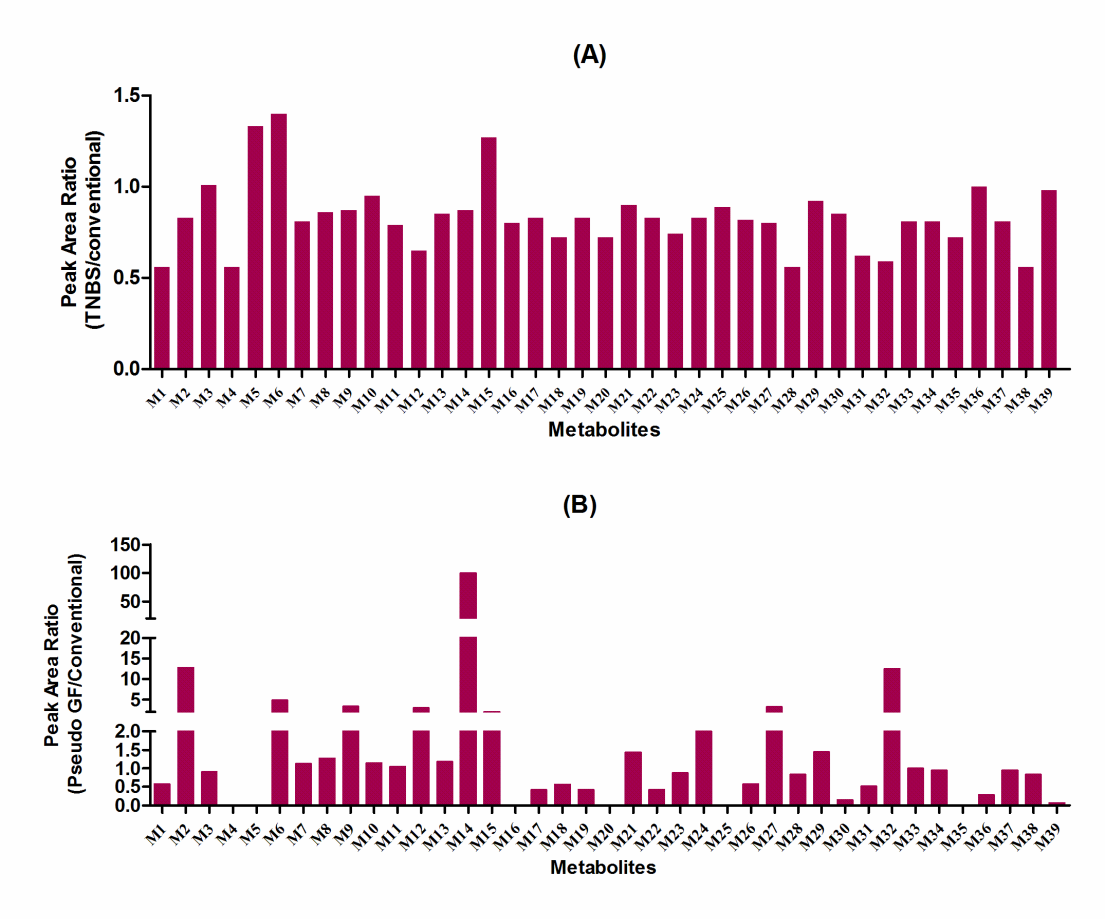

Fig. 5 The average metabolite peak area ratio of Panax notoginseng extract in conventional, TNBS-challenged and pseudo GF rat intestinal microbiota. (A) the average metabolite peak area ratio of TNBS-challenged group and conventional group, (B) the average metabolite peak area ratio of pseudo GF group and conventional group.

4. DISCUSSION

Intestinal microflora, which consists of at least 1000 species of microorganisms together with a variety of yeasts and microorganisms residing in or passing through the gastrointestinal tract, plays major roles in health and disease such as maturation of the immune system (Mazmanian et al., 2005; Wilson and Nicholson, 2009; Shoaib et al., 2015) and response to epithelial cell injury. Importantly, intestinal microflora could produce different metabolic profiles compared with other organs due to its unique enzymes and transporters for oral administrated substances with poor

membrane permeability and bioavailability (Niu et al., 2013). Panax notoginseng are usually administered orally, after which their complicated components (PNSs) contact with intestinal microflora and are metabolized by the enzyme expressed in gut microbiota (Xu et al., 2014, Wang et al., 2014). Their deglycosylated products formed by bacterial conversion always have higher bioavailability and bioactivity (Shen et al. 2013). Thus, the metabolic investigation of Panax notoginseng in intestinal tract is necessary for elucidating its pharmacological activities.

In the present study, the metabolism of PPD-type PNSs (ginsenoside Rb1, Rb2 and Rd) and PPT-type PNSs (ginsenoside Re, Rf, Rg1 and notoginsenoside R1) was studied in the conventional, TNBS-challenged and pseudo GF rat gut microflora. The results indicated that no qualitative difference on metabolite identification was detected between the gut microbiota from the conventional and TNBS-challenged groups. Nevertheless, several other metabolites could not be found in the pseudo GF gut microflora. Exposure levels of some metabolites in the TNBS-challenged group were lower than those in the conventional group, and significant quantitative differences of the metabolites were detected between the pseudo GF rat intestinal microflora and the conventional rat intestinal microflora. The Principal Component Analysis (PCA) plots for the GF group clearly deviated from those of the TNBS-challenged and pseudo GF groups, and the metabolism of ginsenoside Rb1, Rb2, Rd, Re, Rf, Rg1 and notoginsenoside R1 were completely separated among the conventional, TNBS-challenged and pseudo GF groups (Fig.S4A). In order to further verify the influence of intestinal microbiota on the metabolism of PNSs, the metabolites of PNE was were qualitative and quantitative analyzed systematically. The PCA plots for the GF group clearly deviated from that of the TNBS and pseudo GF groups, and the metabolism of PNE in rat flora were completely separated among the conventional, TNBS-challenged and pseudo GF groups (Fig.S4B). Most of the metabolites in TNBS-challenged group were identified as the deglycosylation products, and had similar exposure levels with those in the conventional group. In the pseudo GF group, the peak area of metabolites, which formed by loss of glucose, xylose and rhamnose, was significantly lower than that in the conventional group.

For the past few years, some research suggested that the intestinal microflora produced

different types of glycosidases, which dominated the hydrolysis of ginsenosides (Niu et al, 2013). In 2015, Liu et al. reported that deglycosylation of Rb1 by intestinal microbiota was inhibited in diabetic rats, which leads to increase of systemic exposure of Rb1 (Liu et al., 2015). In order to further investigate the effect of bacterial community structure on the deglycosylated metabolism of PNSs, the activities of glycosidases (β-glucosidase and β-xylosidase) in intestinal microbiota were determined in conventional, TNBS-challenged and pseudo GF rat gut microflora using glycosidase assay kits. As shown in Fig. 6A, β-glucosidase activity of intestinal microbiota in the TNBS-challenged group was slightly lower than that in the conventional group, but the difference had no statistical significance. In addition, the activity of β-glucosidase in the pseudo GF group was 2.8 % of that in the conventional group, and great difference was found between pseudo GF group and the conventional group. The activities of β-xylosidase in the three groups are shown in Fig. 6B. Obviously, β-xylosidase activities in microbiota from the TNBS-challenged and pseudo GF groups were much lower than that in the conventional group. The β-xylosidase activity in the TNBS-challenged group was 67.1% of that in the conventional group, and β-xylosidase activity in the pseudo GF group was 25.7 % of that in the conventional group. According to the results above, the activities of glycosidases (β-glucosidase and β-xylosidase) in the TNBS-challenged rats were a little lower than that in the conventional group, and glycosidase activities in the pseudo GF rats were greatly lower than that in the conventional rats. After comparing the bacterial community structure of conventional, TNBS-challenged and pseudo GF rat intestinal microflora, the change trend of the activities of glycosidases were highly correlated with the alteration of proteobacteria. Thus, Proteobacteria was likely to affect the deglycosylated metabolism of PNSs via regulating the activities of glycosidases.

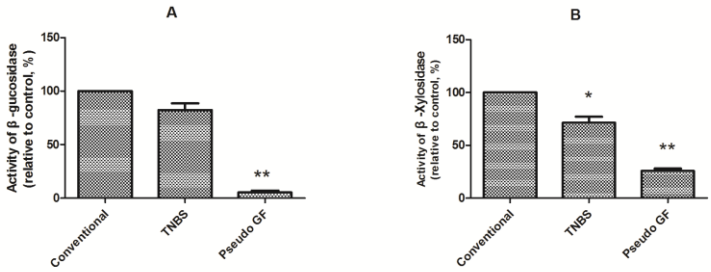

Fig. 6 The activities of glycosidases (β-glucosidase and β-xylosidase) in conventional, TNBS-challenged and

pseudo GF rats. (A) the relative activities of β-glucosidase, (B) the relative activities of β-xylosidase.

Several other types of metabolites, which formed by oxidation, dehydrogenation, demethylation, etc, exhibited higher relative exposure in pseudo GF rats than those in the conventional and TNBS-challenged rats. After comparing with the bacterial community structure with the relative exposure of the metabolites, the population of Bacteroidetes was found to have good relation with the amount of metabolites. Thus, the up-regulation of Bacteroidetes, especially Bacteroides, Erysipelatoclostridium and Blautia, could enhance the activities of redox enzymes in rat intestinal microbiota. In future studies, the effect of Bacteroidetes on the activities and expression of redox enzymes will be further investigated.

Acknowledgments

This study was supported by the National Nature Science Foundation (81273589, 81573559, 81374054, 81530098), the nature science foundation of Jiangsu province (BK20131311), the outstanding youth fund of State Key Laboratory of Natural Medicines (SKLNMZZJQ201602).

Conflict of interest

The authors declare that there is no potential conflict of interest.

Reference

Avershina, E., Frisli, T., Rudi, K., 2013. De novo semi-alignment of 16S rRNA gene sequences for deep phylogenetic characterization of nextgeneration sequencing data. Microbes environment 28, 211-216.

Caporaso, J.G., Kuczynski, J., Stombaugh, J., Bittinger, K., Bushman, F.D., Costello, E.K., Fierer, N., Peña, A.G., Goodrich, J.K., Gordon, J.I., Huttley, G.A., Kelley, S.T., Knights, D., Koenig, J.E., Ley, R.E., Lozupone, C.A., McDonald, D., Muegge, B.D., Pirrung, M., Reeder, J., Sevinsky, J.R., Turnbaugh, P.J., Walters, W.A., Widmann, J., Yatsunenko, T., Zaneveld, J., Knight, R., 2010. QIIME allows analysis of high-throughput community

sequencing data. Nature methods 7, 335-336.

Caporaso, J.G., Lauber, C.L., Walters, W.A., Berg-Lyons, D., Lozupone, C.A., Turnbaugh, P.J., Fierer, N., Knight, R., 2011. Global patterns of 16S rRNA diversity at a depth of millions of sequences per sample. Proceedings of the national academy of sciences 108, 4516-4522.

Cui, Q., Pan, Y., Xu, X., Zhang, W., Wu, X., Qu, S., Liu, X., 2016. The metabolic profile of acteoside produced by human or rat intestinal bacteria or intestinal enzyme in vitro employed UPLC-Q-TOF-MS. Fitoterapia 109, 67-74.

De Preter, V., Hamer, H.M., Windey, K., Verbeke, K., 2011. The impact of pre- and/or probiotics on human colonic metabolism: does it affect human health? Molecular nutrition & food research 55, 46-57.

Fan, Y., Qiao, Y., Huang, J., Tang, M., 2016. Protective Effects of Panax notoginseng Saponins against High Glucose-Induced Oxidative Injury in Rat Retinal Capillary Endothelial Cells. Evidence-based complementary and alternative medicine 5326382.

Gerritsen, J., Smidt, H., Rijkers, G.T., de Vos, W.M., 2011. Intestinal microbiota in human health and disease: the impact of probiotics. Genes & nutrition 6, 209-240.

Gong, P., Cui, N., Wu, L., Liang, Y., Hao, K., Xu, X., Tang, W., Wang, G., Hao, H., 2012. Chemicalome and metabolome matching approach to elucidating biological metabolic networks of complex mixtures. Analytical chemistry 84, 2995-3002.

Guadamuro, L., Delgado, S., Redruello, B., Florez, A.B., Suarez, A., Martinez-Camblor, P., Mayo, B., 2015. Equol status and changes in fecal microbiota in menopausal women receiving long-term treatment for menopause symptoms with a soy-isoflavone concentrate. Frontiers in microbiology 6, 777.

Haiser, H.J., Turnbaugh, P.J., 2012. Is it time for a metagenomic basis of therapeutics? Science 336, 1253-1255.

Han, S.Y., Li, H.X., Bai, C.C., Wang, L., Tu, P.F., 2010. Component analysis and free radical-scavenging potential of Panax notoginseng and Carthamus tinctorius extracts. Chemistry biodiversity 7, 383-391.

Jia, X.H., Wang, C.Q., Liu, J.H., Li, X.W., Wang, X., Shang, M.Y., Cai, S.Q., Zhu, S., Komatsu, K., 2013. Comparative studies of saponins in 1-3-year-old main roots, fibrous roots, and rhizomes of Panax notoginseng, and identification of different parts and growth-year samples. Journal of natural medicines 67, 339-349.

Jia, H. R., Geng, L. L., Li, Y. H., Wang, Q., Diao, Q.Y., Zhou, T., Dai, P.L., 2016. The effects of Bt Cry1Ie toxin on bacterial diversity in the midgut ofApis mellifera ligustica (Hymenoptera: Apidae). Scientific reports 6, 24664

Kim, K.A., Yoo, H.H., Gu, W., Yu, D.H., Jin, M.J., Choi, H.L., Yuan, K., Guerin-Deremaux, L., Kim, D.H., 2015. A prebiotic fiber increases the formation and subsequent absorption of compound K following oral administration

of ginseng in rats. Journal of ginseng research 39, 183-187.

Lin, M., Sun, W., Gong, W., Ding, Y., Zhuang, Y., Hou, Q., 2015. Ginsenoside Rg1 protects against transient focal cerebral ischemic injury and suppresses its systemic metabolic changes in cerabral injury rats. Acta pharmaceutica sinica B 5, 277-284.

Liu, C., Hu, M., Guo, H., Zhang, M., Zhang, J., Li, F., Zhong, Z., Chen, Y., Li, Y., Xu, P., Li, J., Liu, L., Liu, X., 2015. Combined contribution of increased intestinal permeability and inhibited deglycosylation of ginsenoside Rb1 in the intestinal tract to the enhancement of ginsenoside Rb1 exposure in diabetic rats after oral administration. Drug Metab Dispos 43, 1702-1710.

Magoč, T., Salzberg, S. L., 2011. FLASH: fast length adjustment of short reads to improve genome assemblies. Bioinformatics 27, 2957-2963.

Mazmanian, S.K., Liu, C.H., Tzianabos, A.O., Kasper, D.L., 2005. An immunomodulatory molecule of symbiotic bacteria directs maturation of the host immune system. Cell 122, 107-118.

Niu, T., Smith, D.L., Yang, Z., Gao, S., Yin, T., Jiang, Z.H., You, M., Gibbs, R.A., Petrosino, J.F., Hu, M., 2013. Bioactivity and bioavailability of ginsenosides are dependent on the glycosidase activities of the A/J mouse intestinal microbiome defined by pyrosequencing. Pharmaceutical research 30, 836-846.

Nicholson, J.K., Holmes, E., Wilson, I.D. 2005. Gut microorganisms, mammalian metabolism and personalized health care. Nature reviews microbiology 3, 431-438.

Qiu, J., 2007. 'Back to the future' for Chinese herbal medicines. Nature reviews drug discovery 6, 506-507.

Shen, H., Leung, W.I., Ruan, J.Q., Li, S.L., Lei, J.P., Wang, Y.T., Yan, R., 2013. Biotransformation of ginsenoside Rb1 via the gypenoside pathway by human gut bacteria. Chinese medicine 8, 22.

Shoaib, A., Dachang, W., Xin, Y., 2015. Determining the role of a probiotic in the restoration of intestinal microbial balance by molecular and cultural techniques. Genetics and molecular research 14, 1526-1537.

Sousa, T., Paterson, R., Moore, V., Carlsson, A., Abrahamsson, B., Basit, A.W., 2008. The gastrointestinal microbiota as a site for the biotransformation of drugs. International journal of pharmaceutics 363, 1-25.

Stojancevic, M., Bojic, G., Salami, H.A., Mikov, M., 2014. The Influence of Intestinal Tract and Probiotics on the Fate of Orally Administered Drugs. Current issues in molecular biology 16, 55-68.

Tu, Y., 2011. The discovery of artemisinin (qinghaosu) and gifts from Chinese medicine. Nature medicine 17,1217-1220.

Wallace, B.D., Wang, H., Lane, K.T., Scott, J.E., Orans, J., Koo, J.S., Venkatesh, M., Jobin, C., Yeh, L.A., Mani, S.,

Redinbo, M.R., 2010. Alleviating cancer drug toxicity by inhibiting a bacterial enzyme. Science 330, 831-835.

Wang, H.Y., Hua, H.Y., Liu, X.Y., Liu, J.H., Yu, B.Y., 2014. In vitro biotransformation of red ginseng extract by human intestinal microflora: metabolites identification and metabolic profile elucidation using LC-Q-TOF/MS. Journal of Pharmaceutical and Biomedical Analysis 98, 296-306.

Wang, X., Wang, H., Zhang, A., Lu, X., Sun, H., Dong, H., Wang, P., 2012. Metabolomics study on the toxicity of aconite root and its processed products using ultraperformance liquid-chromatography/electrospray-ionization synapt high-definition mass spectrometry coupled with pattern recognition approach and ingenuity pathways analysis. Journal of proteome research 11, 1284-1301.

Wilson, I.D., Nicholson, J.K., 2009. The role of gut microbiota in drug response. Current pharmaceutical design 15, 1519-1523.

Xie, P.S., Leung, A.Y. 2009. Understanding the traditional aspect of Chinese medicine in order to achieve meaningful quality control of Chinese materia medica. Journal of chromatography A. 1216, 1933-1940.

Xing, R., Zhou, L., Xie, L., Hao, K., Rao, T., Wang, Q., Ye, W., Fu, H., Wang, X., Wang, G., Liang, Y., 2015. Development of a systematic approach to rapid classification and identification of notoginsenosides and metabolites in rat feces based on liquid chromatography coupled triple time-of-flight mass spectrometry. Analytica chimica acta. 867, 56-66.

Xu, R., Peng, Y., Wang, M., Fan, L., Li, X., 2014. Effects of broad-spectrum antibiotics on the metabolism and pharmacokinetics of ginsenoside Rb1: a study on rats gut microflora influenced by lincomycin. Journal of ethnopharmacology 158, 338-344.

Yu, Y., Sun, G., Luo, Y., Wang, M., Chen, R., Zhang, J., Ai, Q., Xing, N., Sun, X., 2016. Cardioprotective effects of Notoginsenoside R1 against ischemia/reperfusion injuries by regulating oxidative stress- and endoplasmic reticulum stress- related signaling pathways. Scientific reports 6, 21730.

Zhou, S.S., Xu, J., Zhu, H., Wu, J., Xu, J.D., Yan, R., Li, X.Y., Liu, H.H., Duan, S.M., Wang, Z., Chen, H.B., Shen, H., Li, S.L., 2016. Gut microbiota-involved mechanisms in enhancing systemic exposure of ginsenosides by coexisting polysaccharides in ginseng decoction. Scientific reports 6, 22474.

Graphical Abstract